# Understanding the properties of interfaces between organic self-assembled monolayers and noble metals – A theoretical perspective

**ARTICLE** *in* SURFACE AND INTERFACE ANALYSIS · MARCH 2008

Impact Factor: 1.25 · DOI: 10.1002/sia.2645



**4 AUTHORS**, INCLUDING:

Lorenz Romaner
Materials Center Leoben Forschung GmbH
**47** PUBLICATIONS **1,955** CITATIONS
SEE PROFILE

Georg Heimel
Humboldt-Universität zu Berlin
**104** PUBLICATIONS **2,695** CITATIONS
SEE PROFILE

Egbert Zojer
Graz University of Technology
**177** PUBLICATIONS **5,281** CITATIONS
SEE PROFILE

Research Article

SURFACE and INTERFACE ANALYSIS

Received: 14 August 2007 Revised: 17 October 2007 Accepted: 17 October 2007 Published online in Wiley Interscience: 9 January 2008

(www.interscience.com) DOI 10.1002/sia.2645

# Understanding the properties of interfaces between organic self-assembled monolayers and noble metals – a theoretical perspective

**Gerold M. Rangger,[a] Lorenz Romaner,[a] Georg Heimel[b] and Egbert Zojer[a]***

**Highly ordered, self-assembled monolayers (SAMs) on (noble) metal surfaces are of particular importance for both the emerging field of single-molecule electronics as well as for improving the characteristics of more conventional organic (opto)electronic devices. In the first part of this article, we review the microscopic description of electrode work function modification induced by SAMs and the alignment of molecular states relative to the states in the metal. The focus will be on the Ag(111) surface and biphenyl SAMs involving different donor–acceptor head-group substituents. The impact of different docking groups will also be discussed and the results will be compared to previous findings (primarily) for SAMs on Au(111). The second part of the article deals with an in-depth description of charge rearrangements and the hybridization between molecular and metal states by projecting the electronic states of the combined system onto the orbitals of the isolated molecules. Furthermore, the sulfur–silver bond is analyzed by means of a crystal orbital occupation population analysis.** 

**Keywords:** simulation; self-assembled monolayer; metal organic interface; slab calculation; molecular electronics; organic electronics

## Introduction

Over the past decades, self-assembled monolayers (SAMs) of organic molecules chemisorbed on different substrates have attracted significant attention[1–6] due to their wide range of possible applications in the field of plastic and molecular electronics. The ease of preparation and the high structural order of SAMs make them promising candidates for modifying macroscopic surface properties such as wetting or corrosion resistance,[7,8] and a variety of applications has been explored such as nanolithography and chemical sensing.[9,10] Furthermore, for the fabrication of organic electronic devices such as organic field effect transistors (OFETs), the utility of controlling the interface energetics by means of SAMs is well acknowledged.[11] In particular, the modification of the substrate work function ($\Phi$) allows for tuning of charge carrier injection barriers.[12,13] Also, for the field of single-molecule electronics, the use of $\pi$–conjugated molecules on noble metal electrodes is of great interest.[14–16] In such devices, the molecule itself represents the active element, and the energetic alignment of the metal Fermi level ($E_F$) with respect to the frontier molecular orbitals (MOs) governs the transport characteristics.

It has been shown that the chemical structure[11,17,18] of the $\pi$–conjugated molecules forming the SAMs (in particular, electron-rich and electron-poor substituents[18] and the nature of the docking group[11]) affects the level alignment and the modification of the substrate work function in a decisive way. While in the above mentioned studies much emphasis was laid on SAMs on Au(111) substrate,[11,17,18] here we focus on Ag(111) surfaces.

The article is organized as follows: The first part analyzes the electronic structure of a number of biphenyls with different head and docking groups and reviews the discussions of Heimel *et al.*[11,18] with the emphasis here on the Ag(111) surface. First, the situation for the isolated monolayer will be discussed; subsequently, bond formation occurring due to adsorption and the corresponding charge rearrangements are described in real space; this, then, allows to develop a consistent picture of the parameters governing level alignment and the total work function modification.

In the second part, a charge conserving way of projecting the density of states (DOS) onto individual MOs, of the adsorbed layer, [molecular orbital density of states (MODOS)] will be described and applied to a SAM on Ag(111); finally, the crystal orbital overlap occupation (COOP)[19,20] approach is used to analyze bonding and antibonding contributions related to the S–Ag bond.

## Methodology

The calculations were performed using density functional theory (DFT)-based band-structure calculations. The repeated-slab approach is adopted with the metal substrate represented by five layers of Ag atoms; the SAM is adsorbed on one side of the metal, and a vacuum gap (>20 Å) is introduced between the uppermost atom of the molecule and the next slab. As a reference system, we chose the 4-mercaptobiphenyl on Ag(111) as this allows us to directly compare our results with previous calculations on Au.[11] The head-group substitutions considered include $-NH_2$ (strong donor), –CN (strong acceptor), and –SH (to have the symmetric

* *Correspondence to: Egbert Zojer, Institute of Solid State Physics, Graz University of Technology, Petersgasse 16, A-8010 Graz, Austria. E-mail: egbert.zojer@tugraz.at*

a *Institute of Solid State Physics, Graz University of Technology, Petersgasse 16, A-8010 Graz, Austria*

b *Department of Material Science and Engineering, Massachusetts Institute of Technology, 77 Massachusetts Ave., Cambridge, MA 02139-4307, USA*

molecule). Moreover, an isocyanate (–NC) docking group has been considered. To describe the various SAMs, we will use the following nomenclature: (docking group |2P| substituent).[11]

The molecules were arranged in a $p(\sqrt{3} \times 3)$ herringbone structure on the substrate as shown in Fig.1. The same arrangement was assumed for all substituents and docking groups to ensure comparability, although it cannot be excluded that electrostatic repulsion[18] somewhat limits the packing density for the two polar end groups $-NH_2$ and –CN. Upon adsorption, the thiols were converted into thiolates with the sulfur atoms bonded to the surface. As previously suggested, we take the fcc-hollow (slightly shifted to the bridge) site as the favorable absorption site.[21,22]

Most calculations were done with the Vienna *ab initio* Simulation Package (VASP) code[23–26] using the PW91 exchange-correlation functional. A plane-wave basis set with a cutoff energy of 20 Ryd was used. For the valence–core electron interaction, the projector augmented-wave method (PAW)[27,28] was applied, which allowed for the low kinetic energy cutoff for the plane-wave basis set. For all SAM-calculations, we used a $(8 \times 5 \times 1)$ Monkhorst–Pack grid[29] of *k*-points for the self-consistent field calculations together with a Methfessel–Paxton occupation scheme[30] (broadening of 0.2 eV). All calculations were done in a non spin-polarized manner; no significant changes are observed in spin-polarized test calculations on similar SAMs on Au(111).[18] All atoms of the molecule as well as of the two upper metal layers were fully relaxed using a damped molecular dynamics scheme until the remaining forces were smaller than 0.01 eV/Å. The atomic orbital-projected density of states (AODOS) in VASP was determined by the projection of each Kohn–Sham orbital onto spherical harmonics inside spheres around each atom and by weighing the contribution of that atomic orbital to the DOS accordingly. To obtain the DOS projected onto the SAM (PDOS), all nonmetallic contributions were summed up.

SIESTA (Spanisch Initiative for Simulations with Thousands of Atoms)[31] calculations were performed as described in Ref. [32]. These calculations are required for obtaining the COOP and MODOS as detailed below. In spite of the methodological differences between the VASP and SIESTA calculations, the deviations between the obtained DOS of the whole system are negligible. This applies also to the respective projected density of states (PDOS) onto the molecular region, which justifies the use of two conceptionally slightly different computational approaches in one study. The big advantage of using SIESTA is that, as a result of the AO type basis set, the calculations of the COOP and MODOS become much more straightforward. Also here, all calculations were done in a non spin-polarized manner. Owing to the fact that there are two molecules per unit cell, this is expected to provide a reasonable description of the situation also when considering the nonsaturated monolayer.

All 3D graphical representations of the system were produced using XCrysDen.[33]

## Results and Discussion

Upon adsorption of a SAM on a metal substrate, the electronic structure of the metal and the SAM are modified. This gives rise to (i) a modification of the work function ($\Delta\Phi$), and (ii) a change in the relative alignment of the molecular states relative to the metal Fermi level (Sections on Isolated SAM, Bond Formation, and Combined System). This is concomitant with a change in the occupation of the MOs of the monolayer (Section on MODOS) and a modification of the bonding–antibonding character between the S–H and S–Ag bonds as analyzed by the COOP.

### Isolated SAM

The conceptional aspects concerning the electronic structure of the SAM on the metal can be best derived from a gedankenexperiment: The first step is the formation of an isolated saturated monolayer (consisting only of the molecules that are already in the geometry they will adopt upon adsorption on the metal; in the case

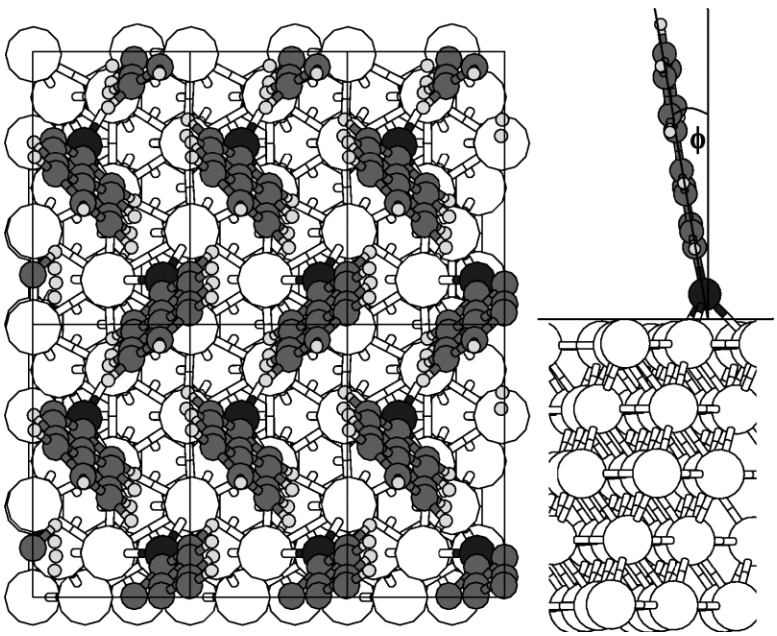


**Figure 1.** Left: Top view of the system. The herringbone structure is well resolved, and the $p(\sqrt{3} \times 3)$ unit cell is indicated by the rectangles. Right: Side view indicating the tilt of the molecules relative to the surface normal. For the various substituents, the inter-ring twist varies between 3° and 5°. The relatively small value can be rationalized by the about 5% higher lateral packing density on the Ag(111) surface compared to the bulk crystal.



  

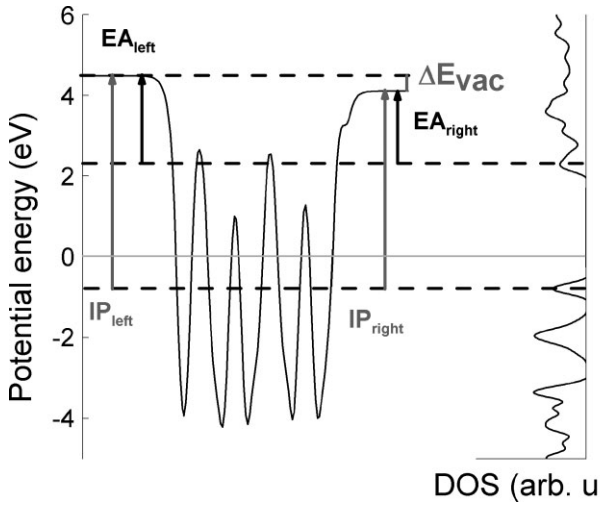


**Figure 2.** Plane-averaged electron potential energy of the (HS|2P|H) monolayer. The different values for $IP_{left}$, $EA_{left}$ and $IP_{right}$, $EA_{right}$ as well as $\Delta E_{vac}$ are indicated. On the right side, the density of states (DOS) of the monolayer is shown clearly revealing the peaks associated with the HOMO and LUMO.

of the thiol docking groups, the S atoms are terminated with H). Figure 2 shows the plane-averaged electrostatic potential of the layer consisting of the saturated molecule (HS|2P|H) together with the DOS. One can identify the energy levels corresponding to the highest occupied molecular orbitals (HOMO) and lowest unoccupied molecular orbitals (LUMO). The vacuum levels to the left and right of the potential well differ by $\Delta E_{vac}$ as the molecules possess an intrinsic dipole moment. Consequently, there are also left and right electron affinities (EAs) and ionization potentials (IPs), as indicated in Fig. 2. In the noninteracting Schottky–Mott limit, $\Delta E_{vac}$ represents the adsorbate-induced work function modification.

Interestingly, although the molecules with different head-group substitutions have significantly different molecular IPs and EAs,[18] their left IPs in the monolayer are virtually identical (Table 1). This behavior is reflected by the fact that the potential distributions in the region of the molecular cores are basically identical for all molecules, i.e. the head-group substitutions influence the plane-averaged potential only in the immediate vicinity of the substituent.[18] Consequently, in the noninteracting Schottky–Mott limit, the positions of the HOMOs relative to the metal Fermi level are the same for (HS|2P|H), (HS|2P|SH), (HS|2P|CN), and (HS|2P|$NH_2$). In contrast, changing the docking group primarily affects the 'left' quantities, while the 'right' ones hardly change,[11] as can be seen for the examples of (HS|2P|H) and (CN|2P|H) in Table 1.

**Table 1.** H-saturated SAMs. Ionization potentials ($IP_{left}$, $IP_{right}$) and electron affinities ($EA_{left}$ and $EA_{right}$) of the (saturated) 2D infinite layer of molecules and step in the potential energy of the electrons across the infinite molecular layer in eV

| Isolated monolayer | $\Delta E_{vac}$ | $IP_{left}$ | $IP_{right}$ | $EA_{left}$ | $EA_{right}$ |
|---|---|---|---|---|---|
| (HS\|2P\|H) | −0.38 | 5.28 | 4.90 | 2.20 | 1.82 |
| (HS\|2P\|NH2) | −1.48 | 5.11 | 3.63 | 2.20 | 0.72 |
| (HS\|2P\|CN) | 3.84 | 5.18 | 9.02 | 2.35 | 6.19 |
| (HS\|2P\|SH) | 0.20[a] | 5.08 | 5.28 | 2.21 | 2.41 |
| (CN\|2P\|H) | −3.47 | 8.53 | 5.06 | 5.45 | 1.98 |

[a] The observation that the nominally symmetric (HS|2P|SH) system also has a nonvanishing $\Delta E_{vac}$ is a result of using the final geometry of the adsorbed monolayer with a slightly distorted geometry for the present considerations.

## Bond formation

In the next step of the gedankenexperiment, the molecular layer is bonded to the Ag surface. For the thiol docking groups, this corresponds to replacing the bond between S and H by a bond between S and three Ag atoms. For the isocyanate docking group, a new bond between the C and the Ag atoms is formed.

The corresponding (plane-averaged) charge rearrangements upon bonding are obtained by subtracting the charge densities of the noninteracting systems, i.e. the Ag slab ($\rho_{Ag(111)}$) and the monolayer ($\rho_{mono}$) (all in their final geometries), from those where the monolayer and the metal interact, i.e. where the charge density of the full system is calculated self-consistently. In the case of thiol docking groups, the isolated monolayer has been saturated with H, which then also needs to be taken into account yielding (*M* denotes the number of molecules in the unit cell):

$$\Delta\rho_{bond}(z) = \frac{1}{M}[\rho(z) - (\rho_{Ag(111)}(z) + \rho_{mono}(z) - \rho_{H}(z))] \qquad (1)$$

$\Delta\rho_{bond}(z)$ for (Ag|S|2P|$NH_2$) is shown in Fig. 3.

One can clearly see that all charge rearrangements are confined to the immediate interface region (i.e. the top two Ag layers as well as the S and the adjacent C atoms). In order to assess the amount of charge transferred upon adsorption, $Q_{bond}$ can be calculated by integrating $\Delta\rho_{bond}$ over z.

$$Q_{bond}(z) = \int_{-\infty}^{z} \Delta\rho_{bond}(z')dz' \qquad (2)$$

The fact that $Q_{bond}$ in the region between the top Ag layer and the S atom becomes zero close to the Au surface and again approaches zero close to the sulfur is an indication for virtually no net charge transfer between the metal and the molecular region.

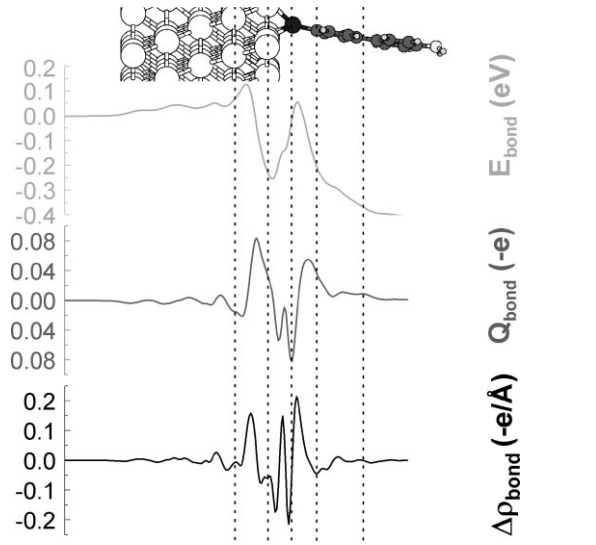


**Figure 3.** Charge rearrangement, $\Delta\rho_{bond}$, and charge transfer, $Q_{bond}$, (definition see text) per molecule as well as the resulting (plane-averaged) potential energy, $E_{bond}$, for the (S|2P|$NH_2$) system. $\Delta\rho_{bond}$ and $Q_{bond}$ have been integrated over the x-y plane of the respective surface unit cell.

**Table 2.** Combined SAM/Ag(111) system: Work function, $\phi_{right}$, of the SAM-covered Ag(111) surface; work function modification induced by the SAM, $\Delta\phi$; bond dipole BD; ionization potential and electron affinity of the molecular layer $IP_{SAM}$ and $EA_{SAM}$; energy corrections for the frontier MOs resulting from adsorption $E_{corr}^{HOMO}$ and $E_{corr}^{LUMO}$; and postions of the frontier $\pi$ and $\pi^*$ states of the SAM relative to the Fermi level $\Delta E_{HOPS}$ and $\Delta E_{LUPS}$. All quantities are given in eV

| System | $\phi_{right}$ | $\Delta\phi$ | BD | $IP_{SAM}$ | $EA_{SAM}$ | $E_{corr}^{HOMO}$ | $E_{corr}^{LUMO}$ | $\Delta E_{HOPS}$ | $\Delta E_{LUPS}$ |
|---|---|---|---|---|---|---|---|---|---|
| Ag\|S\|2P\|H | 3.71 | −0.73 | −0.39 | 4.88 | 1.77 | 0.01 | 0.4 | −1.17 | 1.93 |
| Ag\|S\|2P\|NH2 | 2.58 | −1.87 | −0.38 | 3.61 | 0.64 | 0.03 | 0.10 | −1.03 | 1.94 |
| Ag\|S\|2P\|CN | 7.93 | 3.48 | −0.35 | 9.00 | 6.13 | 0.03 | 0.07 | −1.07 | 1.80 |
| Ag\|S\|2P\|SH | 4.28 | −0.18 | −0.37 | n.a | n.a | n.a | n.a | n.a. | n.a. |
| Ag\|CN\|2P\|H | 2.85 | −1.64 | 1.82 | 5.26 | 2.41 | −0.19 | −0.43 | −2.41 | 0.44 |

This is in sharp contrast to SAMs at reduced packing densities where a pronounced maximum of $Q_{bond}$ is observed in that region.[34] As charge rearrangements are also associated with changes in the potential landscape, the modification of the electrostatic potential upon bond formation, $V_{bond}(z)$, can be obtained by solving the Poisson equation:

$$\frac{d^2V_{bond}}{dz^2} = -\frac{\theta}{\varepsilon_0 A}\Delta\rho_{bond} \tag{3}$$

The potential energy of the electron, $E_{bond} = -eV_{bond}(z)$, where $-e$ denotes the electron charge, is also shown in Fig.3. The net change of the potential energy resulting from the bond is ~0.4 eV and will be referred to in the following as bond dipole (BD). As there is no net long range charge transfer, its appearance can be associated with the charge fluctuations represented by $\Delta\rho_{bond}(z)$ acting like a series of (small) local dipoles. The BD values for the different substituents are summarized in Table 2 and are all found to be very similar. They are consistently smaller by a factor of more than 2 compared to bonding the same molecules to an Au(111) surface.[11] For the isocyanate docking group, a much larger BD is obtained, which even points in the opposite direction, which is again consistent with the observations on Au.[11]

### The combined system: Conjugated SAM on Ag(111)

Owing to the strong localization of $\Delta\rho_{bond}$ in the densely packed system, the potential distribution for the combined system (metal substrate + SAM) can, in a first approximation, be regarded as a the potential of the bare Ag slab plus as the potential of the molecular layer shifted by BD. The actual, self-consistently calculated situation is shown in Fig. 4 for the (Ag|S|2P|H) system. Again, the positions of the states in the SAM can be derived from the corresponding PDOS. The assignment of PDOS features to individual MOs is, however, not always straightforward in the interacting case (especially for (Ag|S|2P|SH))[11]. Therefore, the terms HOPS (highest occupied $\pi$-state) and LUPS (lowest unoccupied $\pi$-state) will be used for the first peaks of the PDOS below and above the Fermi level. The latter characterizes the energy up to which the states in the metal slab are filled. Consequently, the energy differences between $E_F$ and the HOPS ($\Delta E_{HOPS}$) and LUPS ($\Delta E_{LUPS}$) correspond to the hole- and electron-injection barriers into the monolayer.

From the above considerations (in particular, the definition of $\Delta\rho_{bond}$), it becomes clear that the overall modification of the work function resulting from covering the Ag(111) surface with a SAM is obtained as a combination of the effect due to the molecular dipole moments expressed by $\Delta E_{vac}$ and the bond dipole BD[12,13,35]

$$\Delta\phi = BD + \Delta E_{vac} \tag{4}$$

The calculated values of $\Delta\phi$ together with the work functions of the SAM-covered Ag substrate ($\phi_{right}$) obtained with the employed methodology are listed in Table 2. The high values obtained for $\Delta\phi$ can be regarded as an upper limit to the actual (experimental) situation considering the high degree of order and uniformity in the SAM assumed here, which might be difficult to achieve experimentally considering the relatively large molecular dipole moments (vide supra).

Amongst the investigated systems, the largest work function decreases are obtained for (Ag|S|2P|$NH_2$) and (Ag|CN|2P|H), where in the former case, a large negative $\Delta E_{vac}$ and the thiol BD are additive, while in the latter case a particularly large $\Delta E_{vac}$ is partly compensated by the BD of the isocyanate docking group. The resulting $\phi_{right}$ in both the cases are already smaller than 3 eV, but in principle, a further significant reduction of the system work function by combining the CN–docking group with a donating substituent like $-NH_2$ can be expected (however, potentially with additional film forming constraints). The opposite trend in $\phi_{right}$ is observed for the –CN end-group substitution where the SAM

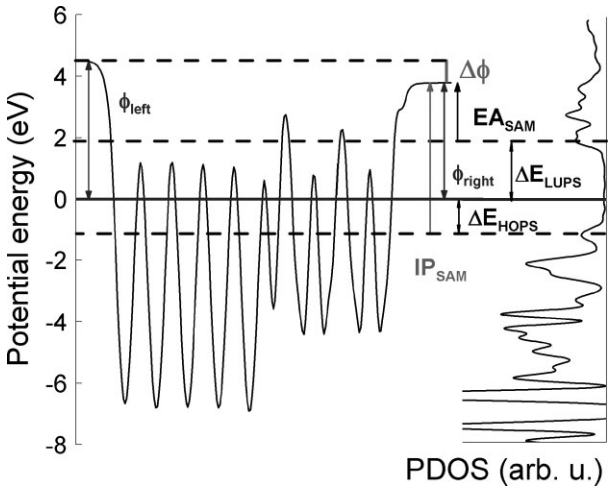


**Figure 4.** Left: Plane-averaged electron potential energy of the combined system (Ag|S|2P|H). Right: Density of states projected onto the molecular region (PDOS); the positions of the HOPS (highest occupied $\pi$-state), and LUPS (lowest unoccupied $\pi^*$-state) are indicated by dashed lines. The IP and EA of the molecular layer ($IP_{SAM}$ and $EA_{SAM}$), the left and right work functions ($\phi_{left}$ and $\phi_{right}$), the work function modification ($\Delta\phi$) as well as the hole- and electron-injection barriers ($\Delta E_{HOPS}$ and $\Delta E_{LUPS}$) are also indicated. The energy scale is given relative to $E_F$.

results in a potential increase of the system work function to nearly 8 eV.

An interesting observation is that when comparing the values of $\phi_{right}$ for the Ag(111) surface in Table 2 with those that can be extracted for Au(111) from Ref. [11], one finds that they are within ~0.2 eV in spite of the fact that the calculated work function of the bare Au(111) surface is 0.7 eV larger than that of Ag(111) ($\phi_{Au(111)} = 5.2$ eV; $\phi_{Ag(111)} = 4.5$ eV). This is because the larger work function of Au is compensated by the equally larger bond dipole (see also discussion for the H-terminated case in Ref. [11]).

The BD also plays a crucial role for the relative alignment between the highest occupied states in the metal at $E_F$ and the molecular levels, as $\Delta E_{HOPS}$ is given by:

$$\Delta E_{HOPS} = \phi_{Au(111)} - IP_{left}^{SAM} + BD + E_{corr} \quad (5)$$

The origin of the (typically relatively small) correction factor, $E_{corr}$, is the slight modification of the potential in the molecular region close to the interface. This results in a small change in the energetic positions of the 'molecular states'. $E_{corr}$ can also be independently calculated from the differences of the 'right' IPs of the isolated monolayers and the layers adsorbed onto the metal.

As far as the level alignment is concerned, it turns out that in the case of the thiol docking group, the frontier molecular $\pi$ and $\pi^*$ states (HOPS and LUPS) are found at virtually the same energetic positions [$(-1.1 \pm 0.1)$eV for the HOPS and $(1.9 \pm 0.1)$eV for the LUPS] independent of whether an electron-rich or an electron-poor substituent is attached to the far end of the molecule. This is analogous to the situation observed for Au(111),[18] although the variations in $\Delta E_{HOPS}$ are somewhat larger here. As can be understood from Eqn. (5), this is a direct consequence of the nearly identical $IPs_{left}$ and BDs obtained for the various end-group substitutions, which result from the strongly localized potential modifications induced by the substituents and also from the local nature of the charge redistributions at the interface (vide supra). In contrast, the large positive BD of the isocyanate docking group increases $\Delta E_{HOPS}$ by nearly 1.3 eV.

Consequently, at least in the densely packed monolayer, an end-group substitution can be used only to control the overall work function of a SAM-covered substrate. Modifying the docking group, however, changes BD, which enters Eqns (4) *and* (5) and, therefore, allows tuning of both, the level alignment as well as the work function modification. After developing this 'general' picture, the following two sections will be dedicated to a more in-depth analysis of MO rearrangements and their contributions to metal–molecule bonding.

### The molecular density of states (MODOS)

When molecules adsorb onto metallic surfaces, interactions occur between the metallic states and the MOs. These interactions cause the MOs to broaden and shift. An explicit way to calculate these effects for the metal–organic interface is to project the DOS onto the MOs.[19,36–41] In this work, this PDOS will be called the MODOS. It identifies the contributions to the total DOS arising from a specific MO, or more precisely, from the band formed by an MO in the isolated monolayer.

The energetic position of the maximum of the MODOS allows determining how a particular MO is aligned with respect to the Fermi level and the broadening of the MODOS is a measure for the hybridization of the corresponding molecular state. It is a measure for the coupling between that particular orbital and with the metallic states. Another purpose of the projection is that, by integrating the MODOS up to the Fermi level, it is possible to assign a nominal occupation to each MO, which allows analyzing the bonding-induced charge transfer for each individual orbital. The methodological concepts used to calculate the MODOS are summarized in the Appendix.

The occupation of each MO can be calculated by integrating the MODOS up to the Fermi level yielding the occupation $O_m$ of the MO.

$$O_m = \int_{-\infty}^{E_f} \mathrm{MODOS}_m(E)dE. \quad (6)$$

The charge associated with each MO then equals $2 \times O_m \times (-e)$.

As a model case, the MODOS for (S|2P|H) on Ag(111) will be discussed. Here, to illustrate the potential of the MODOS for analyzing bonding between a metal and an organic layer, we will primarily describe the situation when considering the nonsaturated (S|2P|H) as the 'reference system'. This provides a more instructive picture, as attaching this layer to the metal results in the formation of a new bond, while in the case discussed in the Section on Isolated SAM, when considering a monolayer saturated with hydrogen, one only deals with replacing one bond (S–H) with another (S–Au).

Prior to adsorption (i.e. in the isolated monolayer) $O_m$ for all 'occupied MOs' is 100%, with the exception of the singly occupied molecular orbital (SOMO), for which it is 50% filled. After adsorption, this occupation pattern is changed as is shown in Fig. 5 (Note: As there are two molecules per unit cell, always two points in the plot correspond to a certain MO). Major changes are observed for the SOMO-6, SOMO-1, and the SOMO, for which we also observe a particularly strong hybridization with the metallic states, as illustrated by the corresponding MODOS plots in Fig. 6 (the MODOS associated with the SOMO-2 is shown for comparison). The contributions of the SOMO-6 and SOMO-1 above the Fermi level (which is set to zero in Fig. 6) cause these orbitals to lose about 0.12 and 0.37 electrons, respectively. The SOMO, on the other hand, gains 0.72 electrons due to the dominant contributions below the

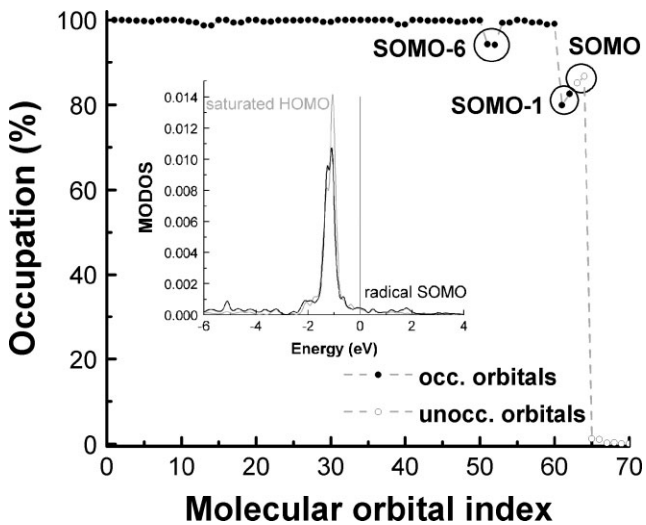


**Figure 5.** Occupation of the molecular orbitals in the SAM/metal system with the unsaturated monolayer taken as the reference. The full (open) circles correspond to the orbitals that are occupied (unoccupied) in the isolated monolayer. The inset compares the MODOS associated with the SOMO (unsaturated monolayer as reference) and the HOMO (saturated monolayer as reference); details see text.

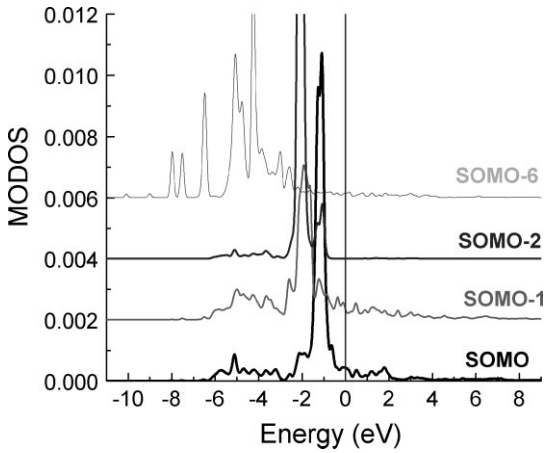


**Figure 6.** MODOS associated with the strongly interacting SOMO-6, SOMO-1, and SOMO orbitals with the unsaturated monolayer taken as the reference. Of each pair of orbitals (resulting from the two molecules in the unit cell of the reference layer; see text), the one at higher energy is plotted. The lower energy one looks very similar. The curves were shifted in y-direction for the sake of clarity. The position of the Fermi energy is taken from the (self-consistent) SIESTA calculations.

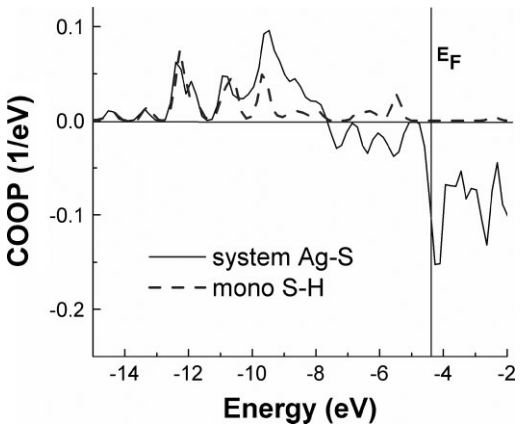


**Figure 7.** COOP (E) between S and all Ag atoms (solid line; combined SAM/metal system) and between S and H (dashed line; saturated monolayer). The position of the Fermi energy is taken from the (self-consistent) SIESTA calculations.

Fermi level (i.e. its maximum being shifted to clearly below the Fermi level as a result of the interaction).

When choosing the monolayer with the sulfur moieties saturated with hydrogen atoms as a reference, no clear trends in the charge redistribution picture can be derived. Rather, all orbitals (including the HOMO, which for this reference system is doubly occupied) lose a varying number of electrons. This is a consequence of the conceptional problem, that, when calculating the MODOS, the hydrogen-related coefficients need to be dropped (as the H atoms are removed upon adsorption). This then results in the 'truncated' MOs becoming linearly dependent. Nevertheless, the resulting MODOS associated with the HOMO in the saturated case is nearly identical to the MODOS of the SOMO in the nonsaturated (i.e. radical) calculations as shown in the inset of Fig. 5.

### The crystal orbital occupation population analysis (COOP)

As a final step, the S–Ag bond is analyzed by means of COOP as described in Ref. [19,20]. This quantity resolves bonding and antibonding contributions to the DOS on the energy scale and is defined as,

$$COOP_{X,Y}(E) = \sum_{m\in X, l\in Y, i, \vec{k}} c^{*}_{im\vec{k}} c_{il\vec{k}} S_{ml\vec{k}} \delta(E - \varepsilon_{i\vec{k}}) \qquad (7)$$

where X and Y denote a set of AOs, typically the AOs belonging to an atom or to a set of atoms (note: as in the case of the MODOS, the COOP is also calculated using SIESTA, which relies on an atomic orbital type basis set). The $c_{il\vec{k}}$ are the corresponding LCAO coefficient and $S_{ml\vec{k}}$ is the overlap matrix. The COOP obeys a sum rule so that $COOP_{X,Y}$ (E) = DOS (E), when X and Y denote the full AO space of the system.

Figure 7 compares the COOP for the S–Ag bond (X= AOs of all Ag atoms and Y= AOs of the two S atoms in the unit cell) and the S–H bond (X= AOs of saturating hydrogen and Y= AOs of sulfur). While at large negative energies the two curves are fully bonding and very similar, differences between the curves arise around the Fermi level of the system. Here the S–Ag bond shows pronounced antibonding contributions, whereas the S–H bond is still bonding. A closer analysis shows that these contributions largely stem from the overlap between the sulfur s-orbitals and the metal states. The total overlap population is obtained via integrating the S–Ag and the S–H COOP up to the Fermi energy. It is an indicator of the strength of a bond. We obtain values of 1.03 and 1.57, respectively; i.e. the S–Ag bond is weaker than the S–H bond due to the antibonding contributions in the energy range up to 3 eV below $E_F$. Interestingly, the ratios between the overlap populations associated with the two bonds (S–Ag/S–H) ~0.65 thus obtained compares well with the ratio of the bond enthalpies of Ag–S ($217\frac{kJ}{mol}$) and S–H ($344\frac{kJ}{mol}$).[42]

## Summary and Conclusions

In summary, we discussed the microscopic origin of the work function modification induced by a SAM chemically bound to a coinage metal as well as the alignment between the molecular and metal states. The former is determined by the sum of the bond dipole and the vacuum level change related to the intrinsic dipole moments of the molecules forming the monolayer; the latter is given by the work function of the isolated monolayer on the side on which it will be attached to the metal plus, again, the bond dipole. Effects resulting from end-group substitution as well as the charge rearrangements following the bonding of the molecules to the surface are strongly localized. Consequently, end-group substitution will only affect the work function modification, while changing the docking group also allows tuning the level alignment. Interestingly, for all investigated SAMs, the work functions for the SAM-covered Ag(111) surfaces are very similar to those for Au(111) as described in Ref. [18].

Moreover, charge rearrangements and hybridization were analyzed on an 'orbital' level by projecting the DOS of the combined molecule/metal system onto the molecular states; the bonding and antibonding overlap populations of the S–Ag and S–H bonds are also compared.

### Acknowledgements

The authors would like to acknowledge the financial support by the European Community project 'Icontrol' (EC-STREP-033197) and by the Austrian Science Foundation (FWF) through the Austrian

Nano Initiative (Project N-702-SENSPHYS). GH is a Marie-Curie fellow under the INSANE project (OIF contract no. 021511). The authors are also grateful to the section 'Computing & Application Services' of the Zentrale Informatikdienst of the Graz University of Technology for providing computational resources and to the Institut für Materialphysik of the Universität Wien for providing the VASP code.

## References

[1] Love JC, Estroff LA, Kriebel JK, Nuzzo RG, Whitesides GM. *Chem. Rev.* 2005; **105**: 1103, DOI: 10.1021/Cr0300789.
[2] Poirier GE. *Chem. Rev.* 1997; **97**: 1117, DOI: 10.1021/cr960074m.
[3] Schreiber F. *Prog. Surf. Sci.* 2000; **65**: 151, DOI: 10.1016/S0079-6816(00)00024-1.
[4] Schreiber F. *J. Phys.: Condens. Matter* 2004; **16**: R881, DOI: 10.1088/0953-8984/16/28/R01.
[5] Schwartz DK. *Annu. Rev. Phys. Chem.* 2001; **52**: 107, DOI: 10.1146/annurev.physchem.52.1.107.
[6] Ulman A. *Chem. Rev.* 1996; **96**: 1533, DOI: 10.1021/cr9502357.
[7] Genzer J, Efimenko K. *Science* 2000; **290**: 2130.
[8] Jennings GK, Laibinis PE. *Colloids Surf. A* 1996; **116**: 105.
[9] Cahen D, Naaman R, Vager Z. *Adv. Funct. Mater.* 2005; **15**: 1571.
[10] Guo XF, Myers M, Xiao SX, Lefenfeld M, Steiner R, Tulevski GS, Tang JY, Baumert J, Leibfarth F, Yardley JT, Steigerwald ML, Kim P, Nuckolls C. *Proc. Natl. Acad. Sci. U.S.A.* 2006; **103**: 11452.
[11] Heimel G, Romaner L, Zojer E, Bredas JL. *Nano Lett.* 2007; **7**: 932, DOI: 10.1021/Nl0629106.
[12] de Boer B, Hadipour A, Mandoc MM, van Woudenbergh T, Blom PWM. *Adv. Mater.* 2005; **17**: 621, DOI: 10.1002/adma.200401216.
[13] Alloway DM, Hofmann M, Smith DL, Gruhn NE, Graham AL, Colorado R, Wysocki VH, Lee TR, Lee PA, Armstrong NR. *J. Phys. Chem. B* 2003; **107**: 11690. DOI:10.1021/Jp034665+.
[14] Chen J, Reed MA, Rawlett AM, Tour JM. *Science* 1999; **286**: 1550.
[15] Bumm LA, Arnold JJ, Cygan MT, Dunbar TD, Burgin TP, Jones L II, Allara DL, Tour JM, Weiss PS. *Science* 1996; **271**: 1705, DOI: 10.1126/science.271.5256.1705.
[16] Kushmerick JG, Holt DB, Yang JC, Naciri J, Moore MH, Shashidhar R. *Phys. Rev. Lett.* 2002; **89**: 086802, DOI: 10.1103/PhysRevLett.89.086802.
[17] Heimel G, Romaner L, Bredas JL, Zojer E. *Surf. Sci.* 2006; **600**: 4548, DOI: 10.1016/j.susc.2006.07.023.
[18] Heimel G, Romaner L, Bredas JL, Zojer E. *Phys. Rev. Lett.* 2006; **96**: DOI: 10.1103/Physrevlett.96.196806.
[19] Hoffmann R. *Rev. Mod. Phys.* 1988; **60**: 601, DOI: 10.1103/RevModPhys.60.601.
[20] Hughbanks T, Hoffmann R. *J. Am. Chem. Soc.* 1983; **105**: 3528, DOI: 10.1021/ja00349a027.
[21] Kim S, Ihm K, Kang T-H, Hwang S, Joo S-W. *Surf. Interface Anal.* 2005; **37**: 294, DOI: 10.1002/sia.2019.
[22] Gottschalck J, Hammer B. *J. Chem. Phys.* 2002; **116**: 784, DOI: 10.1063/1.1424292.
[23] Kresse G, Furthmüller J. *Phys. Rev. B* 1996; **54**: 11169, DOI: 10.1103/PhysRevB.54.11169.
[24] Kresse G, Hafner J. *Phys. Rev. B* 1993; **47**: 558, DOI: 10.1103/PhysRevB.47.558.
[25] Kresse G, Hafner J. *Phys. Rev. B* 1993; **48**: 13115, DOI: 10.1103/PhysRevB.48.13115.
[26] Kresse G, Hafner J. *Phys. Rev. B* 1994; **49**: 14251, DOI: 10.1103/PhysRevB.49.14251.
[27] Blöchl PE. *Phys. Rev. B* 1994; **50**: 17953, DOI: 10.1103/PhysRevB.50.17953.
[28] Kresse G, Joubert D. *Phys. Rev. B* 1999; **59**: 1758, DOI: 10.1103/PhysRevB.59.1758.
[29] Monkhorst HJ, Pack JD. *Phys. Rev. B* 1976; **13**: 5188, DOI: 10.1103/PhysRevB.13.5188.
[30] Methfessel M, Paxton AT. *Phys. Rev. B* 1989; **40**: 3616, DOI: 10.1103/PhysRevB.40.3616.
[31] Soler JM, Artacho E, Gale JD, Garcia A, Junquera J, Ordejon P, Sanchez-Portal D. *J. Phys.: Condens. Matter* 2002; **14**: 2745, DOI: 10.1088/0953-8984/14/11/302.
[32] Romaner L, Heimel G, Gruber M, Bredas JL, Zojer E. *Small* 2006; **2**: 1468, DOI: 10.1002/smll.200600054.
[33] Kokalj A. *Comput. Mater. Sci.* 2003; **28**: 155.
[34] Romaner L, Heimel G, Zojer E. *Phys. Rev. B.* (in press).
[35] Campbell IH, Rubin S, Zawodzinski TA, Kress JD, Martin RL, Smith DL, Barashkov NN, Ferraris JP. *Phys. Rev. B* 1996; **54**: 14321, DOI: 10.1103/PhysRevB.54.R14321.
[36] Hughbanks T, Hoffman R. *J. Am. Chem. Soc.* 1983; **105**: 1150, DOI: 10.1021/ja00343a014.
[37] Ample F, Curulla D, Fuster F, Clotet A, Ricart JM. *Surf. Sci.* 2002; **497**: 139, DOI: 10.1016/S0039-6028(01)01639-9.
[38] Bagus PS, Illas F. *J. Chem. Phys.* 1992; **96**: 8962.
[39] Curulla D, Clotet A, Ricart JM, Illas F. *J. Phys. Chem. B* 1999; **103**: 5246, DOI: 10.1021/jp984802g.
[40] Hauschild A, Karki K, Cowie BCC, Rohlfing M, Tautz FS, Sokolowski M. *Phys. Rev. Lett.* 2005; **94**: 036106, DOI: 10.1103/PhysRevLett.94.036106.
[41] Nelin CJ, Bagus PS, Philpott MR. *J. Chem. Phys.* 1987; **87**: 2170, DOI: 10.1063/1.453142.
[42] Lide DR. *CRC Handbook of Chemistry and Physics 1999–2000: A Ready Reference Book of Chemical and Physical Data* (81st edn). CRC Press: USA, June 6 2000.

## Appendix

A 'straightforward' approach (as adopted, for example, by Nelin *et al*.[41]) for calculating the MODOS would be:

$$MODOS'_m(E) = \sum_{i,\vec{k}} \left|\langle \tilde{M}_{m\vec{k}}|\phi_{i\vec{k}}\rangle\right|^2 \delta(E-\varepsilon_{i\vec{k}}) = \sum_{i,\vec{k},g,h} \left|\tilde{M}^*_{mg\vec{k}} c_{ih\vec{k}} S_{gh\vec{k}}\right|^2 \delta(E-\varepsilon_{i\vec{k}}) \quad \text{(A1)}$$

where the Blochstates of the combined metal/organic system are denoted by $|\phi_{i\vec{k}}\rangle$ and the Bloch states of the isolated monolayer (obtained from a separate calculation) by $|\tilde{M}_{m\vec{k}}\rangle$. $\tilde{M}_{mg\vec{k}}$ and $c_{ih\vec{k}}$ are the corresponding LCAO coefficients, i.e. $|\tilde{M}_{m\vec{k}}\rangle = \sum_g \tilde{M}_{mg\vec{k}}|A_{g\vec{k}}\rangle$ and $|\Phi_{i\vec{k}}\rangle = \sum_h c_{ih\vec{k}}|A_{h\vec{k}}\rangle$ where $|A_{g\vec{k}}\rangle$ denotes the AOs (Bloch). Finally $S_{gh\vec{k}} = \langle A_{g\vec{k}}|A_{h\vec{k}}\rangle$ is the overlap matrix.

The problem arising from this definition is that the overlap of the AOs from the metal with the AOs from the monolayer gives rise to undesired contributions to the MODOS. This is best understood when considering the case where the $|\phi_{i\vec{k}}\rangle$ s are obtained from a calculation where only metal atoms are present. Then, the MODOS according to (A1) would already be nonzero (due to the overlap of the monolayer AOs with the metal AOs) *although no molecule is present in the calculation*. In the work by Nelin *et al*.[41] this undesired 'overlap charge' is eliminated by subtraction.

Following Refs. [19 and 35], we adopt an alternative definition where this problem is completely avoided. It is based on the Mulliken-type partitioning of the DOS as used by the SIESTA code to, e.g. partition the DOS into the contribution of the AOs (AODOS). Applying an analogous definition for the MODOS, we obtain:

$$MODOS_m(E) = \sum_{i,l,\vec{k}} c^{M}_{im\vec{k}}{}^* c^{M}_{il\vec{k}} \hat{S}_{ml\vec{k}} \delta(E-\varepsilon_{i\vec{k}}) \quad \text{(A2)}$$

where $c^{M}_{im\vec{k}}$ are the LCMO coefficients and $\hat{S}_{ml\vec{k}}$ is the overlap matrix of the MO. As the $|\tilde{M}_{m\vec{k}}\rangle$ s are defined only on the monolayer part of the system, they are augmented with the AOs belonging the metal atoms to obtain the new basis set $\{|M_{m\vec{k}}\rangle\}$. The LCMO

coefficients $c^{M}_{im\vec{k}}$ are calculated by solving the linear system

$$\sum_{m} M_{mg\vec{k}} c^{M}_{im\vec{k}} = c_{ig\vec{k}} \tag{A3}$$

where the coefficients $M_{mg\vec{k}}$ form a matrix M with the following structure

$$M = \begin{pmatrix} E & 0 \\ 0 & \tilde{M} \end{pmatrix} \tag{A4}$$

The MODOS has three important properties in contrast to the straightforward projection, namely, (i) the problem with the overlap charge is avoided (ii) summation over all molecular MOs gives exactly the same as summation over all AOs belonging to the monolayer, i.e. the projected molecular DOS (PDOS) can be defined as $PDOS = \sum_{|M_m\rangle \in monolayer} MODOS_m(E) = \sum_{|A_m\rangle \in monolayer} AODOS_m(E)$ (iii) as a consequence of (ii) the Mulliken charge of the monolayer can be partitioned into contributions stemming from the different MOs.